Interference between Selected Dipoles and Octupoles in the Optical Second-Harmonic Generation from Spherical Gold Nanoparticles

J. Butet, G. Bachelier,* I. Russier-Antoine, C. Jonin, E. Benichou, and P.-F. Brevet

Laboratoire de Spectrométrie Ionique et Moléculaire (LASIM), Université Claude Bernard Lyon 1 - CNRS (UMR 5579), Bâtiment A. Kastler, 43 Boulevard du 11 novembre 1918, 69622 Villleurbanne, France

(Received 21 April 2010; published 10 August 2010)

Optical second-harmonic generation from gold nanoparticles is investigated both experimentally and theoretically. The contribution of octupoles is reported for the first time in the second-harmonic emission pattern, by using an harmonic polarization in the scattering plane. The experimental results presented here for particle sizes up to 100 nm are in excellent agreement with finite element method simulations involving the normal surface term only in the nonlinear polarization source. In addition, analytical calculations based on nonlinear Mie scattering theory clearly evidence the constructive and destructive interferences occurring between the dipolar and octupolar responses selected with this polarization configuration.

DOI: 10.1103/PhysRevLett.105.077401 PACS numbers: 78.67.Bf, 42.25.Hz, 42.65.Ky, 73.20.Mf

Noble-metal nanoparticles play a singular role in nanosciences and nanotechnology owing to the well-known surface plasmon polaritons [1] leading to both field localization and enhancement. These two key features have opened extensive applications in surface-enhanced spectroscopies [2] and light guiding and coupling in plasmonic devices and nanoantennas [3,4]. Nowadays, almost any particle shape (spheres, rods, cubes, decahedra) can be obtained owing to the progress in the synthesis of shape-controlled nanocrystals [5]. This allows tailoring the desired spectral response but also the desired particle symmetry, leading to specific near-field distributions of the electromagnetic field. Owing to all these properties, noble-metal nanoparticles have triggered a new and exponentially increasing interest in linear and, more recently, nonlinear optics such as the second-harmonic generation (SHG) phenomenon for almost a decade. The specificity of the second-order nonlinear process is that it is forbidden in the dipolar approximation in centrosymmetric materials, as is the case for noble metals [6]. Hence, the nonlinear response is dominated by the contribution of the metal surface, where the centrosymmetry is broken, and of the bulk owing to field gradients [7]. Metal films and L-shaped structures prepared by lithography were recently investigated by the group of Kauranen [8] evidencing interferences between the two kinds of contributions.

Systematic experimental investigations have also been performed on colloidal solutions allowing the analysis in a homogeneous environment of the intrinsic properties of the metal particles [9–14]. More precisely, the size dependence of the nonlinear efficiency, the effects of the surface plasmon resonances, the composition (gold, silver, or copper), and the homogeneity of the internal structure (alloys or core-shell structures) have been addressed. The SH scattering properties of spherical nanoparticles were found to be dominated by the dipolar and quadrupolar responses (where the multipoles are those of the Mie theory) as evidenced by polarization-resolved measurements. The dipolar response is, in principle, forbidden by symmetry arguments in the specific experimental configuration [15]. Its observation was attributed to the deviation of the exact shape of the particle from the perfect spherical shape [9] and recently confirmed by finite elements methods (FEM) simulations [16], accounting for both polarization and size dependences. An almost pure quadrupolar response has been reported very recently at the single particle level [17].

In this Letter, we investigate further, experimentally and theoretically, the SHG response from approximately spherical gold nanoparticles with hyper-Rayleigh scattering where the SH light is collected at a right angle from the fundamental beam. We report for the first time the observation of an octupolar response in the harmonic field component parallel to the scattering plane for particles as small as 70 nm in diameter. The experimental data are compared to both FEM [16] and analytical [18] simulations, giving a clear picture of the interference phenomenon occurring between the polarization-selected dipolar response, already reported in a few works only [9,19], and this new octupolar contribution. The role of the retardation effects in the interference contrast is, in particular, quantitatively addressed.

We used a mode-locked Ti:sapphire laser tuned to 780 nm and delivering pulses of about 180 fs at a repetition rate of 76 MHz. The average output power was about 800 mW at the laser exit. The polarization angle of the input beam γ is selected with a rotating half-wave plate, $\gamma = 0$ or π corresponding to a vertically polarized incident wave. A red filter was placed in front of it to remove any residual light at the harmonic frequency generated in the wave plate. The fundamental beam is focused into a quartz cell with a microscope objective (16, numerical aperture 0.32). The collection is performed perpendicular to the

incident beam with a 25 mm focal length lens with a numerical aperture of 0.5. The SH photons, the polarization of which is selected by an analyzer, are collected by a cooled photomultiplier after spectral selection performed by a blue filter and a monochromator. A mechanical chopper on the fundamental beam allows the rejecting of undesirable photons coming from the environment. This experimental setup has recently been used to performed hyper-Rayleigh scattering from metallic nanoparticles with very low concentrations, ultimately where a single nanoparticle is located in the focal volume of the beam [20]. The gold nanoparticle aqueous solutions were purchased and used as received (BBI international).

Horizontally analyzed second-harmonic measurements (electric field in the scattering plane) have been reported in the past for small spherical [9] and flat triangular [19] metallic nanoparticles only. The corresponding SH intensity was found to be independent of the incident polarization angle as expected for the excitation of an electric dipole at the harmonic frequency arising either from the noncentrosymmetry of the particles randomly distributed into the liquid aqueous phase [16] or from the spatial variation of the fundamental electric field over the nanoparticles [15]. In the latter case, in particular, this dipole is aligned with the fundamental beam propagation axis, and its amplitude is independent of the input polarization angle for spherical particles. It therefore leads to a constant SH intensity. Figure 1 shows horizontally analyzed SH measurements as a function of the input polarization for 50 and 100 nm gold nanoparticles. As expected, the results obtained for the 50 nm diameter gold nanoparticles are independent of the input polarization in agreement with the dipolar emission properties discussed above [9,15,16]. In contrast, the horizontally analyzed SH intensity for 100 nm gold nanoparticles reaches a maximum value for vertically polarized input electric fields ($\gamma = 0$ or π). This additional contribution increases in amplitude as the particle size increases. It is therefore likely related to retardation effects.

Additional measurements were performed for 20 and 80 nm nanoparticles evidencing a smooth evolution of the polar graphs as a function of the particle size (data not shown). All SH emission patterns were perfectly fitted with the following equation:

$$I^H_{HRS} = a^H \cos^4\gamma + b^H \cos^2\gamma \sin^2\gamma + c^H \sin^4\gamma, \quad (1)$$

where the parameters a^H, b^H, and c^H are real coefficients. For horizontally analyzed SHG with constant amplitude, the γ dependence in Eq. (1) vanishes owing to the relation $2a^H = 2c^H = b^H$ [21]. For nonconstant SH emission patterns, this equality no longer holds. Since the deformed polar plots exhibit maxima at $\gamma = 0$ or π, as shown in Fig. 1, the parameter a^H becomes larger than c^H. Hence, the deviation from a pure dipolar response corresponding to a constant horizontally analyzed SH intensity can be quantified by the single parameter $\zeta^H = (a^H - c^H)/(a^H + c^H)$. Its dependence on the diameter of the gold nanoparticle is shown in Fig. 2. As expected, this ratio vanishes for gold particles smaller than 50 nm as their response is dominated by a pure dipolar contribution. It, however, increases with the particle size up to 0.16 for 100 nm diameter gold nanoparticles. As shown in Fig. 2, the deviation from a pure dipolar SH response starts to be effective (larger than the experimental uncertainty) for nanoparticles as small as 70 nm.

To characterize this new contribution to the SHG response in large noble-metal nanoparticles, FEM simulations were performed as reported in Ref. [16]. Briefly, the

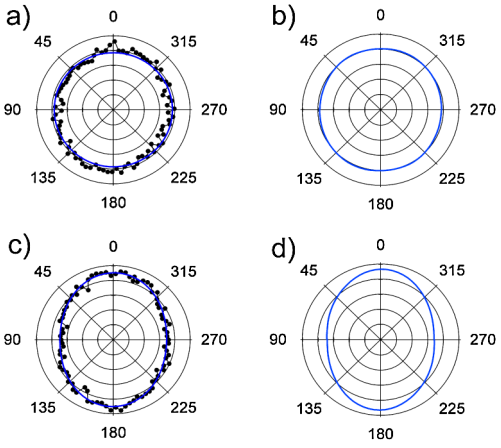

FIG. 1 (color online). Horizontally analyzed SH intensity as a function of the input polarization for 50 (a),(b) and 100 nm (c), (d) gold nanoparticles. The experimental data are shown with filled circles (a),(c) and fitted by using Eq. (1) (plain curves). The corresponding FEM simulations are shown in the right-hand panel (b),(d).

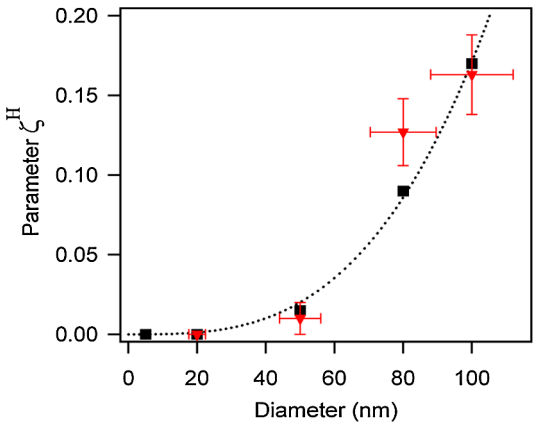

FIG. 2 (color online). Parameter ζ^H as a function of the gold nanoparticle diameter as experimentally measured (red triangles) and calculated by using FEM simulations (black squares). The dotted line is a fit of the simulated data with the equation Ad^p, where d is the nanoparticle diameter. The vertical and horizontal error bars are obtained from the fitting procedure and the size dispersion, respectively.

field distribution at the fundamental frequency excited by the incident beam is determined first; see Figs. 3(a) and 3(b). It is then used to calculate the nonlinear sources associated with the surface quadratic susceptibility tensor component $\chi^{(2)}_{s,nnn}$. Maxwell's equations are solved in a second step by using the weak formulation in order to obtain the near-field distribution of the fields at the harmonic frequency; see Figs. 3(c) and 3(d). As shown in Figs. 3(a) and 3(b), the retardation effects at the fundamental wavelength are very weak for both 50 and 100 nm nanoparticles, the linear optical properties being largely dominated by the dipolar response. In contrast, the near-field distribution of the SH electric field strongly differs for 50 and 100 nm gold nanoparticles. It clearly shows that retardation effects at the emission step are prominent for the larger particles [see Fig. 3(d)] as evidenced by the asymmetry of the near-field map and the distortion of the multipolar lobes. The far-field scattered intensity, which can be compared to the experimental data, is calculated from the near-field distribution of the SH field by using the Stratton-Chu formula [16]. As shown in Fig. 1, the deviation from a constant horizontally polarized SH intensity is very well reproduced by the FEM simulation for both the orientation and the amplitude of the deformation. The experimental results presented here can therefore be accounted for with FEM simulations including the normal quadratic susceptibility surface term only. Additional FEM simulations, not shown here, were performed with deformed particles [16]. As a matter of fact, a constant intensity was also obtained as a function of the input polarization for weakly deformed particles. This latter simulation confirms that the deformation of the SH emission patterns experimentally observed cannot be explained by the deviation of the nanoparticles shape from that of a perfect sphere.

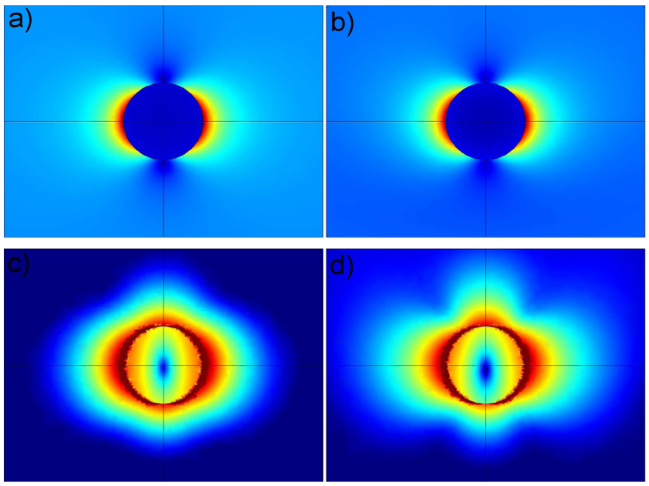

FIG. 3 (color online). Calculated near-field distribution for the fundamental (a),(b) and harmonic (c),(d) electric fields for 50 (a),(c) and 100 nm (b),(d) gold nanoparticles. The image plane is given by the incident electric field, aligned with the dipolar lobes (a),(c), and the corresponding wave vector. The harmonic fields are shown in a logarithmic scale.

The parameter ζ^H determined from the FEM simulations is reported in Fig. 2, pointing out that calculated SH responses and experimental measurements are in excellent agreement. A fitting procedure with the function Ad^p, where d is the nanoparticle diameter and A and p are the parameters, leads to a variation of the parameter ζ with the third power of the nanoparticle diameter ($p = 3.01 \pm 0.02$). From the size dependence of this additional contribution, one cannot directly infer the nature of the additional multipole involved. One way to answer this question would have been to project the harmonic near field obtained with the FEM simulations on the different multipolar surface plasmon modes. Instead, we follow an analytical approach in order to establish a link with previous theoretical works.

Following the notation introduced by Dadap and coworkers [15], the more efficient mechanism leading to a dipolar SH emission for a perfect sphere is $E1 + E2 \rightarrow E1$, where the two terms on the left of the arrow refer to the nature of the interaction with the fundamental wave and the third term describes that of the SH emission. Explicitly, this notation corresponds to a dipolar emission ($E1$) coming from the combination of an electric dipole ($E1$) and an electric quadrupole ($E2$) excitation. The $E1 + E1 \rightarrow E1$ mechanism is forbidden for centrosymmetric objects, since this channel violates parity conservation. In addition to the well-known $E1 + E1 \rightarrow E2$ channel, there is a third possibility involving electric dipoles ($E1$) and quadrupoles ($E2$) and satisfying the conservation of the angular momentum. This mechanism, corresponding to a $E1 + E2 \rightarrow E3$ contribution, was not previously taken into account in the small-particle limit [15] but has to be considered where larger particles are involved. This octupolar term ($E3$) appears as a good candidate to account for the observed deformation of the SH intensity pattern and is related to retardation effects.

In order to establish the role of each multipole in the SH response and confirm the octupolar origin of the additional contribution in the nonconstant SH intensity pattern, analytical calculations were performed by using the nonlinear Mie scattering model developed by Pavlyukh and Hübner [18]. After determining the multipole expansion for the fundamental field inside the sphere, the SH surface sources were computed by using Clebsch-Gordan algebra. The appropriate formulation for the boundary conditions applied to the harmonic field is still under discussion [22]. Nevertheless, the symmetry of the excited multipoles is well accounted for by the present calculation and leads to a clear and simple interpretation of the experimental data.

By using surface nonlinear sources given by $\chi^{(2)}_{s,nnn}$, very simple selection rules are obtained. The vertically E^V_l and horizontally E^H_l polarized harmonic fields are nonzero for angular momenta l even and odd, respectively, as discussed

by Dadap *et al.* [15]. Hence, in our experimental configuration and for the surface nonlinear source $\chi^{(2)}_{s,nnn}$, odd and even plasmon modes are decoupled and can be independently selected in vertically or horizontally analyzed measurements. This would not be the case in other configurations such as that used in Ref. [23] due to the presence of the substrate and the scattering angle. The following expressions for the far-field SH electric field can be deduced from Ref. [18]:

$$E_1^H = \alpha, \tag{2}$$

$$E_3^H = \kappa + \eta\cos(2\gamma), \tag{3}$$

where α, κ, and η are three functions of the nanoparticle diameter and the gold dielectric constants at the fundamental and the harmonic frequencies. Obviously, the equality $2a^H = 2c^H = b^H$ is now broken with the introduction of the term E_3^H, which is the only one depending on the incident polarization angle. The deviation from a pure dipolar SH response leading to a variation of the horizontally analyzed SH intensity with the input polarization angle is therefore due to the electric octupolar term as anticipated above. The constant term $\alpha + \kappa$ arises from both the dipolar and the octupolar fields, and therefore it cannot be separated into its two components. However, the ratio between the oscillating and the constant parts, namely, the ratio $\eta/(\alpha + \kappa)$, is found to be 8% for 100 nm gold particles, evidence of an already significant contribution of the octupole contribution to the scattered SH intensity for this particle size.

The dipolar and the octupolar modes both contribute to the horizontally polarized SH electric field. Therefore, they do interfere in the far-field region. The deformation of the polar plot shown in Fig. 1 can hence be analyzed in terms of constructive interferences for the maxima of the SH intensity at the angles $\gamma = 0$ and π and destructive interferences at the angles $\gamma = \pi/2$ and $3\pi/2$. Rotating the polarization of the fundamental electric field allows exploring the entire interference patterns. In this context, the parameter ζ^H finds a natural interpretation if recast in the following form:

$$\zeta^H = \frac{I^H_{\max} - I^H_{\min}}{I^H_{\max} + I^H_{\min}}. \tag{4}$$

Clearly, ζ^H translates the interference contrast between the dipolar and the octupolar plasmon modes selected in our specific experimental configuration. As the particle size increases, the amplitude of the octupolar contribution increases owing to the retardation effects, leading to a growing interference contrast with the dipolar contribution.

In summary, octupolar SHG from spherical gold nanoparticles is reported for the first time. This contribution starts to be effective for nanoparticles as small as 70 nm in diameter. Owing to the setup geometry we used where the fundamental input and the scattered output directions are at a right angle, even and odd multipolar contributions to the total SH response can be independently selected by using orthogonal analyzers. The octupolar contribution is revealed in the horizontally analyzed SH intensity configuration through to its interference with the dipolar one. The interference contrast is controlled by the input polarization and shown to increase with the particle volume. All experimental observations are in excellent agreement with FEM simulations. The pioneering combination of FEM simulations and analytical models provides furthermore a clear understanding of the characteristics of the SH emission from noble-metal nanoparticles.

*Corresponding author.
guillaume.bachelier@lasim.univ-lyon1.fr

[1] A. V. Zayats, I. I. Smolyaninov, and A. A. Maradudin, Phys. Rep. **408**, 131 (2005).
[2] K. Kneipp *et al.*, Phys. Rev. Lett. **78**, 1667 (1997).
[3] P. Muhlschlegel, H. J. Eisler, O. J. F. Martin, B. Hecht, and D. W. Pohl, Science **308**, 1607 (2005).
[4] J. C. Weeber, A. Dereux, C. Girard, J. R. Krenn, and J. P. Goudonnet, Phys. Rev. B **60**, 9061 (1999).
[5] Y. Xia, Y. J. Xiong, B. Lim, and S. E. Skrabalak, Angew. Chem., Int. Ed. **48**, 60 (2009).
[6] R. W. Boyd, *Nonlinear Optics* (Academic, New York, 1992).
[7] S. S. Jha, Phys. Rev. **140**, A2020 (1965).
[8] S. Kujala, B. K. Canfield, M. Kauranen, Y. Svirko, and J. Turunen, Phys. Rev. Lett. **98**, 167403 (2007).
[9] J. Nappa *et al.*, Phys. Rev. B **71**, 165407 (2005).
[10] I. Russier-Antoine, E. Benichou, G. Bachelier, C. Jonin, and P. F. Brevet, J. Phys. Chem. C **111**, 9044 (2007).
[11] I. Russier-Antoine *et al.*, Phys. Rev. B **78**, 035436 (2008).
[12] E. C. Hao, G. C. Schatz, R. C. Jonhson, and J. T. Hupp, J. Chem. Phys. **117**, 5963 (2002).
[13] R. C. Johnson, J. Li, J. T. Hupp, and G. C. Schatz, Chem. Phys. Lett. **356**, 534 (2002).
[14] M. Chandra and P. K. Das, Chem. Phys. **358**, 203 (2009).
[15] J. I. Dadap, J. Shan, K. B. Eisenthal, and T. F. Heinz, Phys. Rev. Lett. **83**, 4045 (1999); J. I. Dadap, J. Shan, and T. F. Heinz, J. Opt. Soc. Am. B **21**, 1328 (2004).
[16] G. Bachelier, I. Russier-Antoine, E. Benichou, C. Jonin, and P. F. Brevet, J. Opt. Soc. Am. B **25**, 955 (2008).
[17] J. Butet *et al.*, Nano Lett. **10**, 1717 (2010).
[18] Y. Pavlyukh and W. Hübner, Phys. Rev. B **70**, 245434 (2004).
[19] A. K. Singh *et al.*, Chem. Phys. Lett. **481**, 94 (2009).
[20] J. Duboisset *et al.*, J. Phys. Chem. C **113**, 13 477 (2009).
[21] S. Brasselet and J. Zyss, J. Opt. Soc. Am. B **15**, 257 (1998).
[22] A. G. F. de Beer and S. Roke, Phys. Rev. B **79**, 155420 (2009).
[23] M. D. McMahon, R. Lopez, R. F. Haglund, Jr., E. A. Ray, and P. H. Bunton, Phys. Rev. B **73**, 041401(R) (2006).